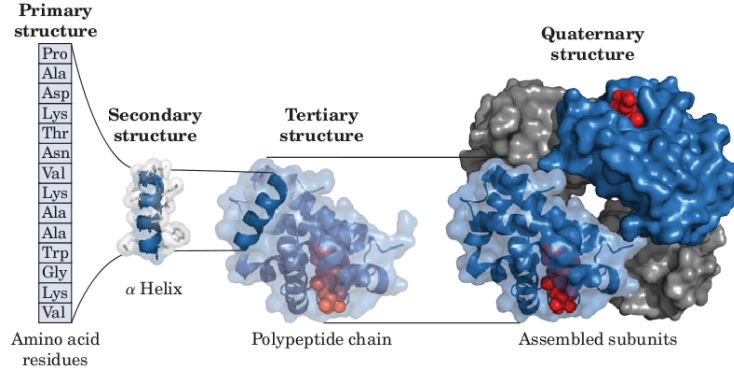


A Deep-Reinforcement Learning Approach to Protein Folding

Conrad Li, Benjamin Beal, Tyler Miller

Proteins: The Building Blocks of Life

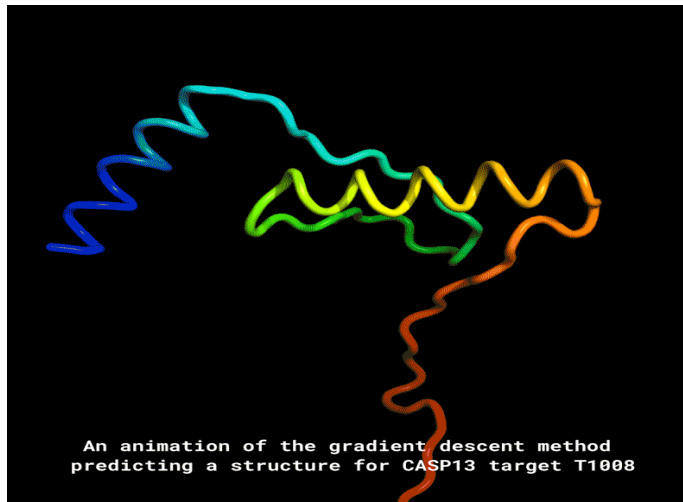
- Proteins are macromolecules in organisms that provide a variety of essential roles for life (i.e. enzyme, structure, transport, messengers, antibodies...)
- Proteins are composed of a sequence of the 20 amino acids
- Proteins have structural hierarchy (primary, secondary, tertiary, quaternary)
- A protein's function is highly dependent on its 3D structure



[Image Source](#)

The Protein Folding Problem

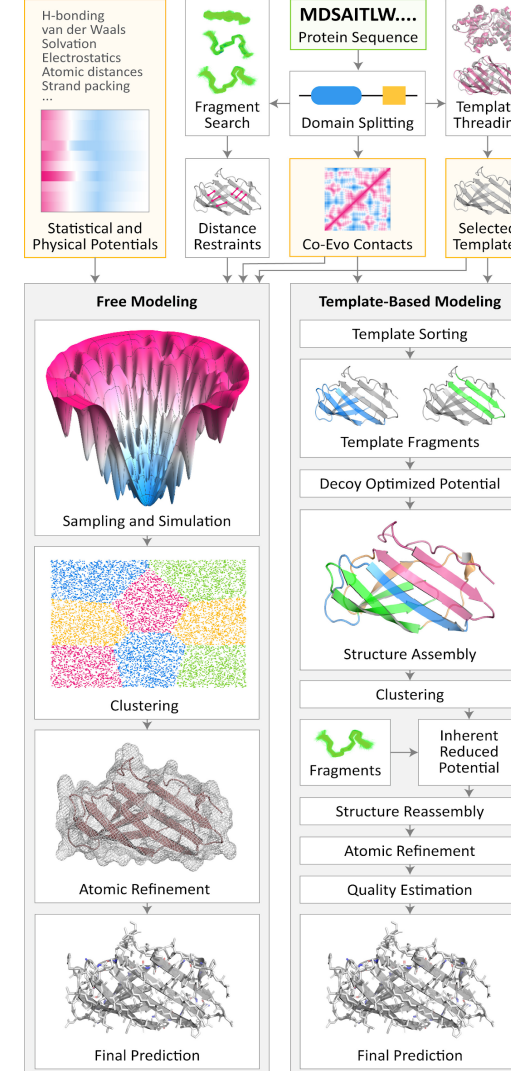
- Predict the 3D structure of a protein given its amino acid sequence
- One may interested in not only the final 3D structure, but also gaining insights into the process of folding itself
- Can be used to speed up drug discovery and discovering new proteins



- Computational protein structure prediction methods can be separated into two categories
- Methods in the first category build explicit sequences to structure maps
 - Molecular dynamics simulations from first principles which are computationally costly)
 - Template-based methods which rely on similarities to previously discovered structures
- Methods in the second category use co-evolution techniques (necessitating a large amount of homologs) to predict distance and/or contact maps

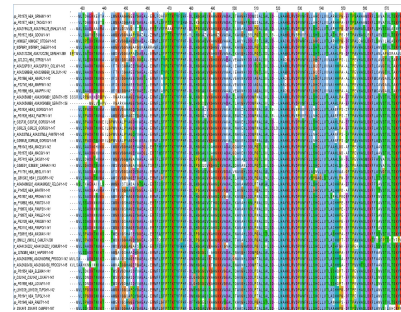
Conventional Pipelines for Protein Structure Prediction

(AIQuraishi, 2019)



RaptorX-Contact

MSA

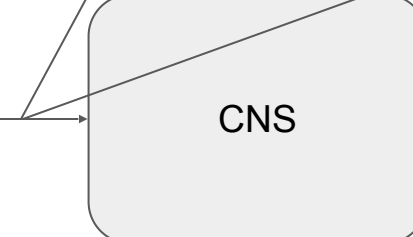
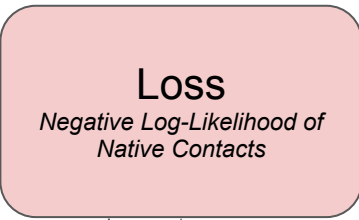


Sequential
Features
 $L \times 26$

Pairwise
Features
 $L \times L \times 3$

L = Sequence Length

$$R_\theta : \mathbb{R}^{L \times 26}, \mathbb{R}^{L \times L} \rightarrow \mathbb{R}^{3 \times L}$$



$$\begin{bmatrix} 0 & d_{12} & d_{13} & \dots & d_{1L} \\ d_{21} & 0 & \ddots & \ddots & \vdots \\ d_{31} & \ddots & 0 & \ddots & \vdots \\ \vdots & \ddots & \ddots & 0 & \vdots \\ d_{L1} & \dots & \dots & \dots & 0 \end{bmatrix}$$

Residue 1 Residue 2

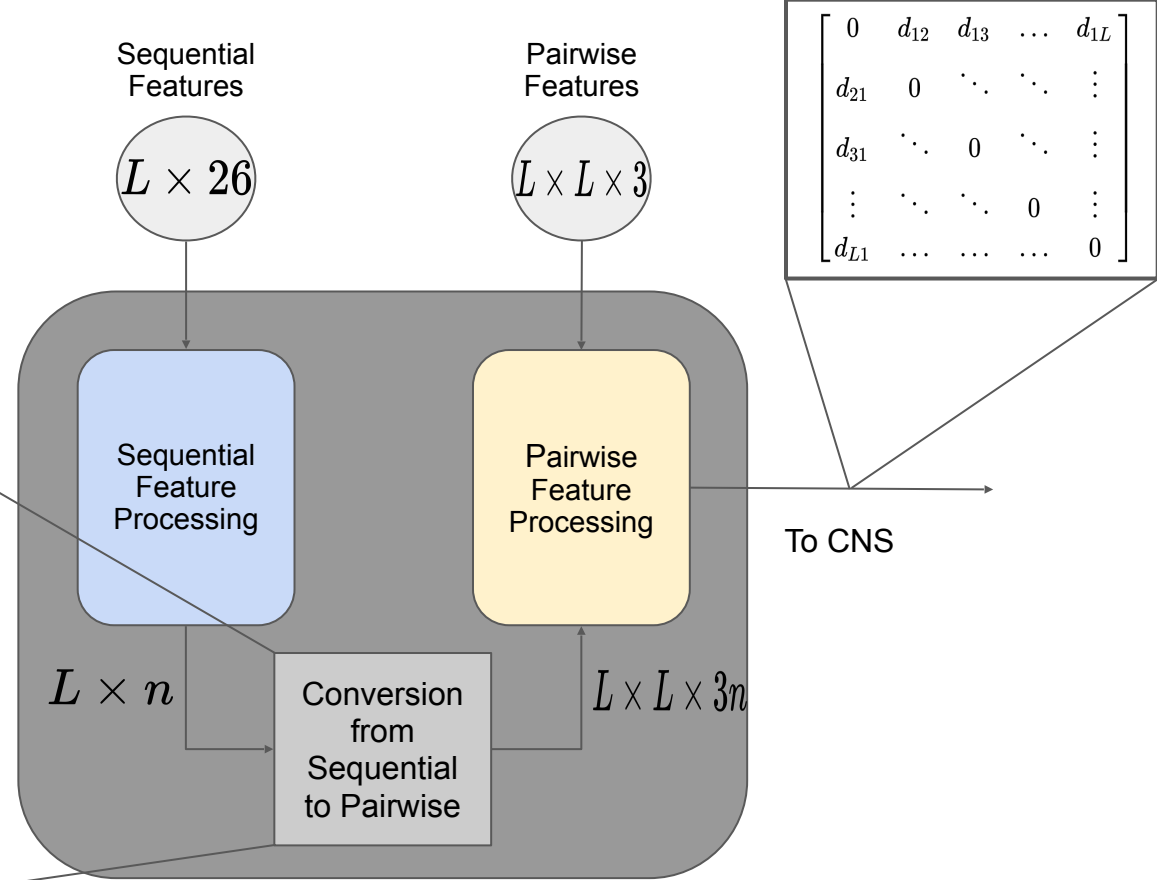
$$\begin{bmatrix} \overbrace{x_1 \ x_2 \ x_3}^{\text{Residue 1}} \ \overbrace{x_4 \ x_5 \ x_6}^{\text{Residue 2}} \ \dots \\ y_1 \ y_2 \ y_3 \ y_4 \ y_5 \ y_6 \ \dots \\ z_1 \ z_2 \ z_3 \ z_4 \ z_5 \ z_6 \ \dots \end{bmatrix}$$

RaptorX-Contact

$$X_\theta : \mathbb{R}^{L \times 26}, \mathbb{R}^{L \times L} \rightarrow \mathbb{R}^{L \times L}$$

v_i = Sequential Output Feature for the i th residue

$$w_{ij} = \begin{bmatrix} v_i \\ v_{\frac{i+j}{2}} \\ v_j \end{bmatrix}$$

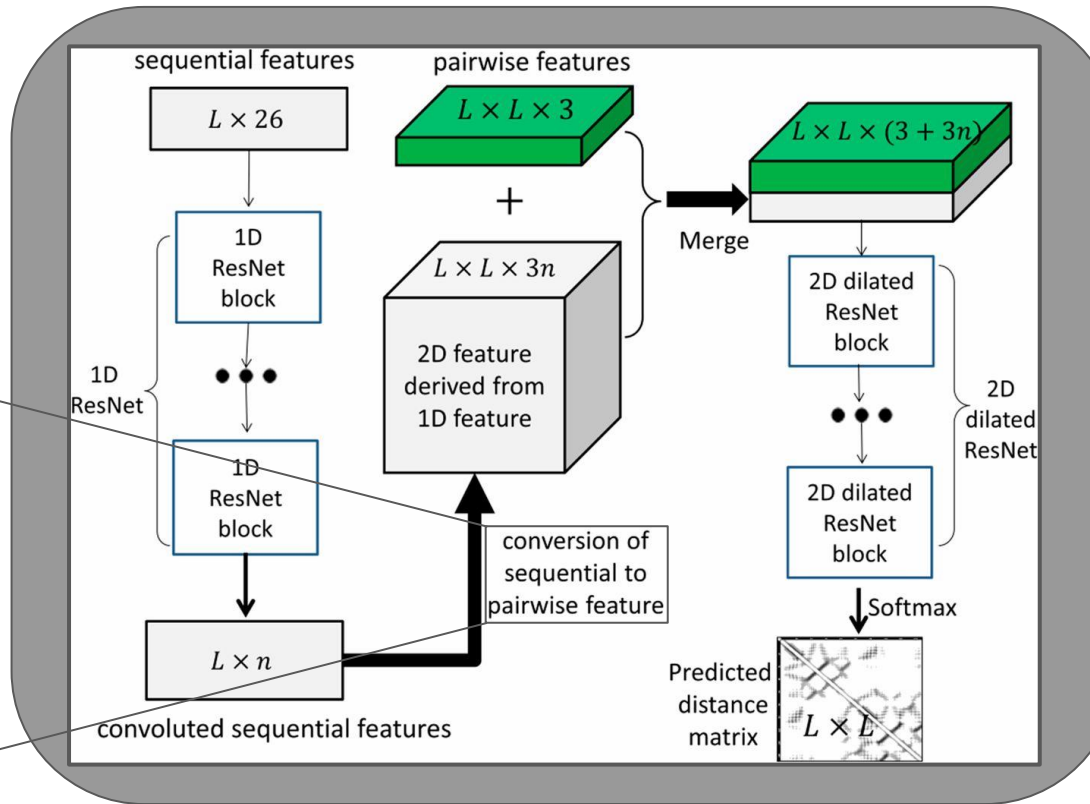


A more detailed examination (See [here](#) for ResNets)

$$X_\theta : \mathbb{R}^{L \times 26}, \mathbb{R}^{L \times L} \rightarrow \mathbb{R}^{L \times L}$$

v_i = Sequential Output Feature for the i th residue

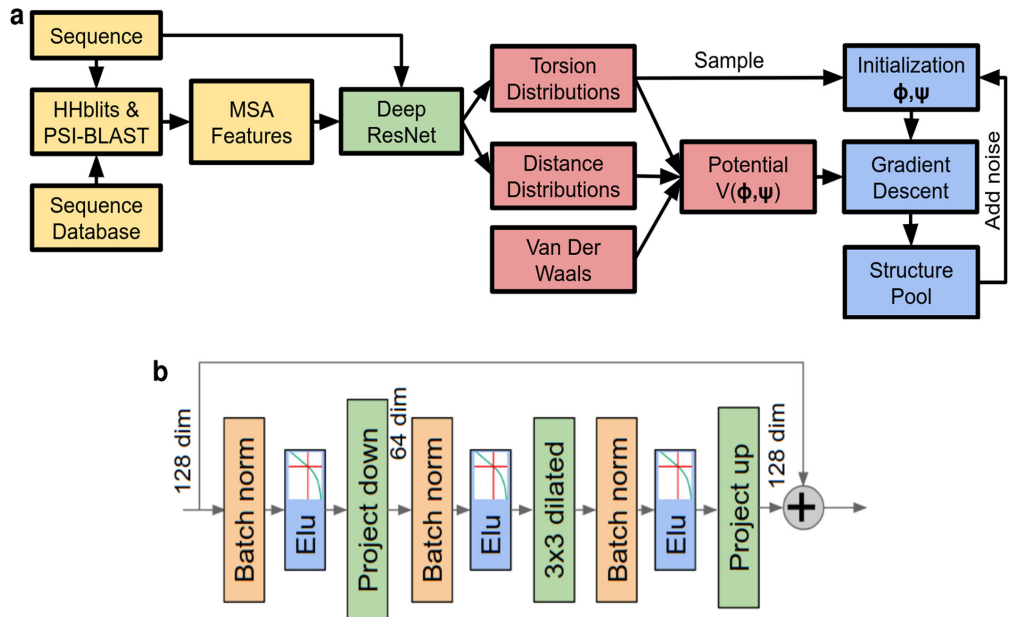
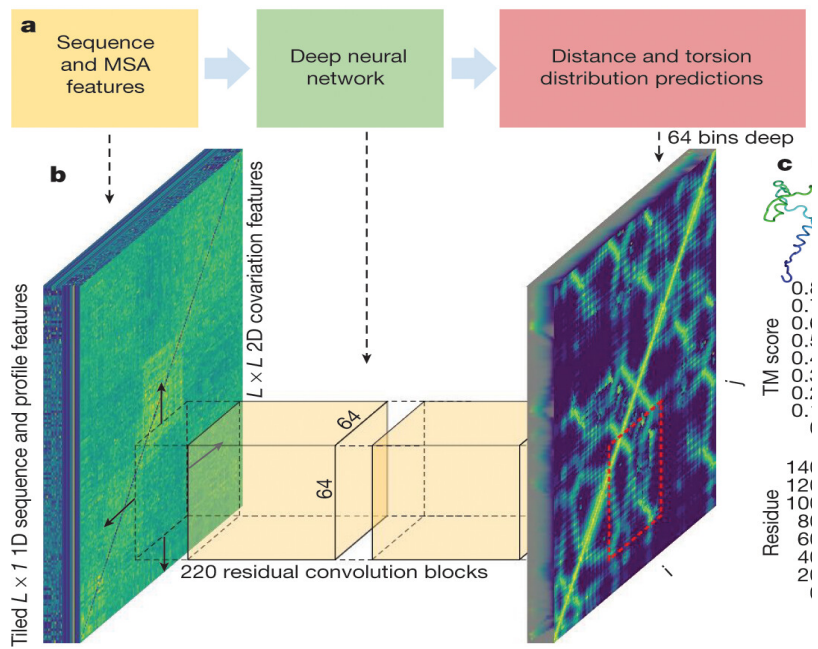
$$w_{ij} = \begin{bmatrix} v_i \\ v_{\frac{i+j}{2}} \\ v_j \end{bmatrix}$$



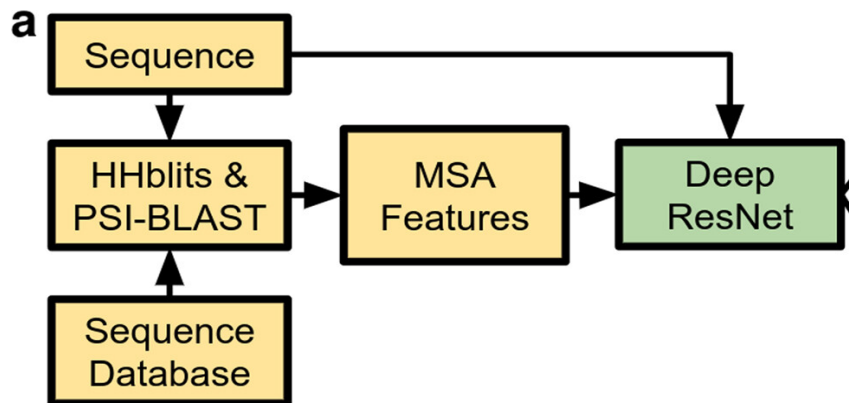
RaptorX-Contact Observations

- Outperforms existing DCA and template based approaches
- Does not directly yield 3D coordinates/model of protein - but can still construct 3D models without involving extensive conformational sampling using CNS
- Model quality directly correlated with MSA depth, logarithm of M_{eff} ($R \approx 0.6$)
- Heavy reliance on co-evolution data prevents it from exploring the full protein design space
- Assumed probability of having a distance $>16 \text{ \AA}$ is 0 which leads to errors

AlphaFold



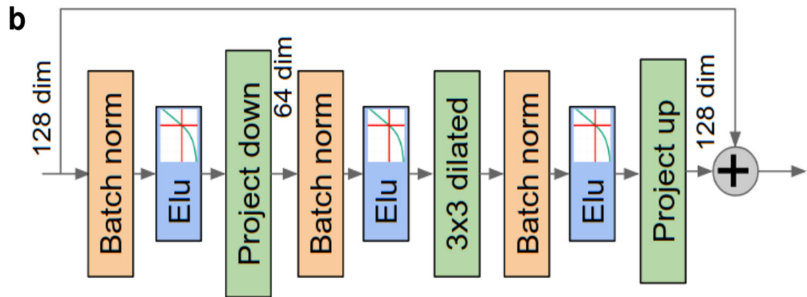
Input Representation



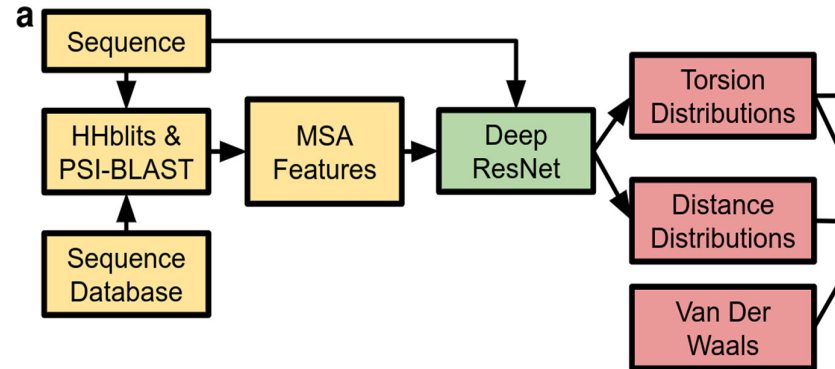
- HHblits alignments ($L \times 1$)
- One hot AA encoding ($L \times 21$)
- PSI-Blast profile ($L \times 21$)
- HHblits profile ($L \times 22$)
- Non-gapped profile ($L \times 21$)
- HMM profile ($L \times 30$)
- Potts model bias ($L \times 22$)
- Deletion probability ($L \times 1$)
- Residue indices ($L \times 1$)
- Potts model parameters ($L \times L \times 484$)
- Norm of potts parameters ($L \times L$)
- Gap matrix ($L \times L$)

Computation/Function

- The network takes the concatenated MSA features and sequence encoding as inputs
- Deep ResNet consists of 220 blocks such as the one shown below



- The network learns a probability distribution of distances between residue pairs ($L \times L \times 64$)
- Trained/tested on 64×64 regions of entire $L \times L$ distogram



Outputs and Learning

- The torsion and distance distributions, along with a Van Der Waals term, were used to construct a distance potential (shown below)

Distance potentials The basic distance potential is computed as a sum over all residue pairs of the likelihood of the inter-residue distances:

$$V_{\text{distance}}(\mathbf{x}) = - \sum_{i,j, i \neq j} \log P(d_{ij} | \mathcal{S}, \text{MSA}(\mathcal{S})). \quad (1)$$

The distance potential with a reference state becomes:

$$V_{\text{distance}}(\mathbf{x}) = - \sum_{i,j, i \neq j} \log P(d_{ij} | \mathcal{S}, \text{MSA}(\mathcal{S})) - \log P(d_{ij} | \text{length}, \delta_{\alpha\beta}). \quad (2)$$

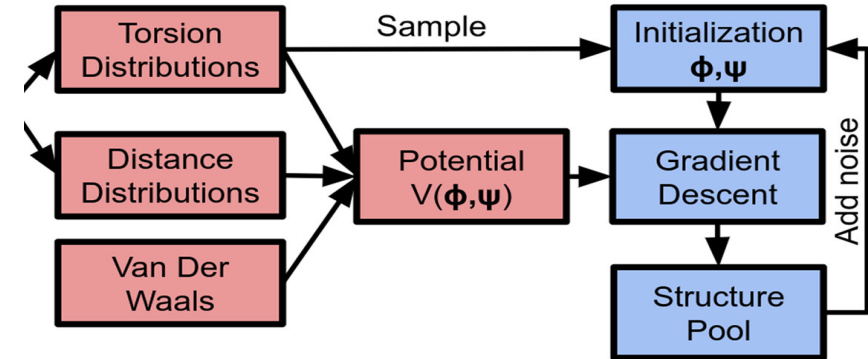
The torsions are modelled with a von Mises distribution for each residue:

$$V_{\text{torsion}}(\phi, \psi) = - \sum_i \log p_{\text{vonMises}}(\phi_i, \psi_i | \mathcal{S}, \text{MSA}(\mathcal{S})). \quad (3)$$

The total potential that we optimise is thus:

$$V_{\text{total}}(\phi, \psi) = V_{\text{distance}}(G(\phi, \psi)) + V_{\text{torsion}}(\phi, \psi) + V_{\text{score2.smooth}}(G(\phi, \psi)). \quad (4)$$

The terms are weighted equally as determined by cross-validation.



- Stochastic Gradient Descent is then used to find a set of torsion angles that minimizes this potential (shown above)

AlphaFold (Pros and Cons)

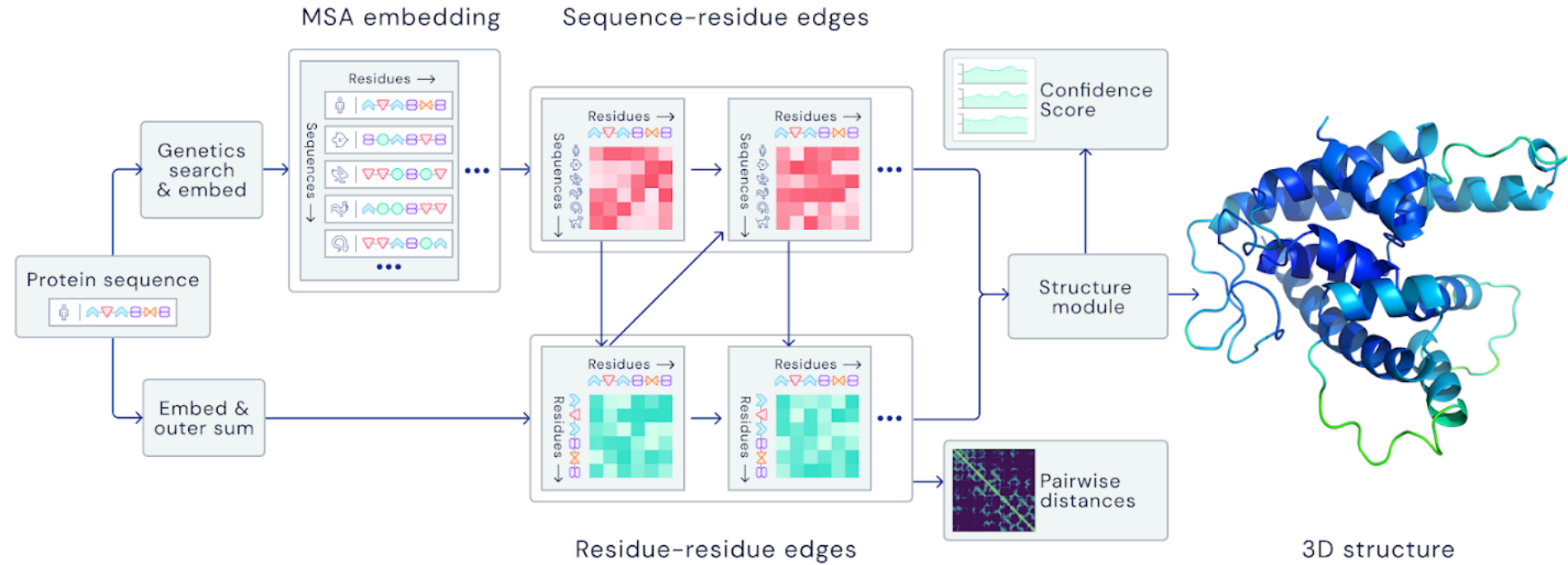
Pros:

- Achieves high accuracy even with few sequence homologs
- Unprecedented FM accuracy
- Matches performance of template-based approaches without using a template

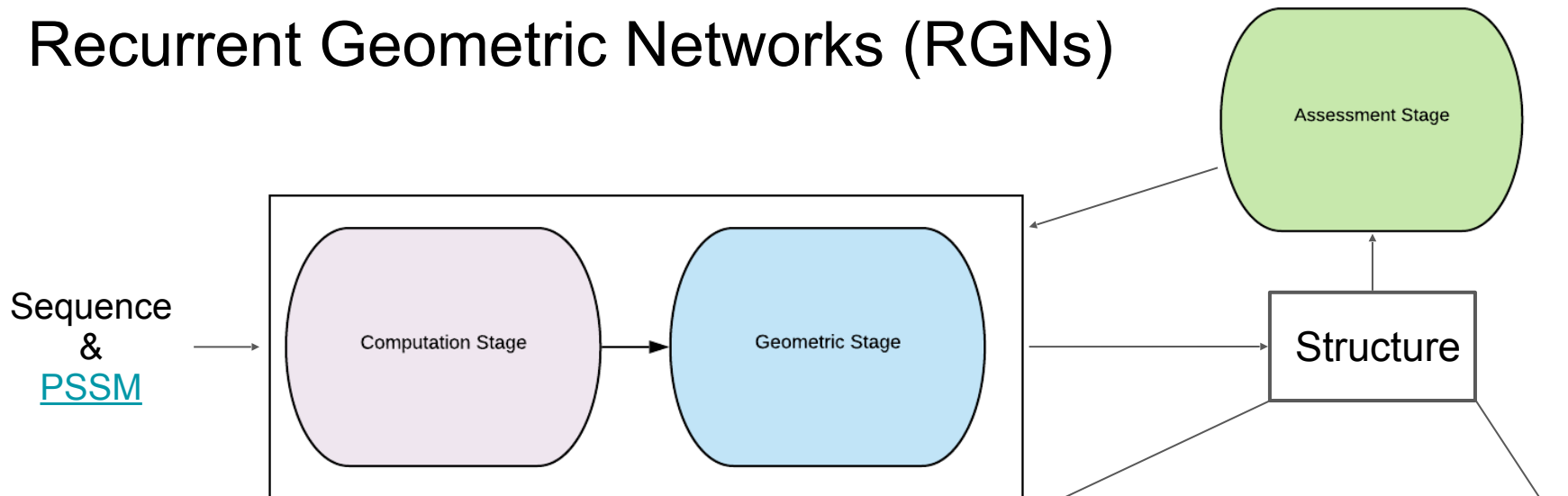
Cons:

- Relies on a complex structure prediction pipeline that must be carefully designed
- Deep learning is applied to only a portion of the pipeline (e.g. predicting the distances) so the entire model is not strictly differentiable and relies on careful feature representation

AlphaFold 2.0

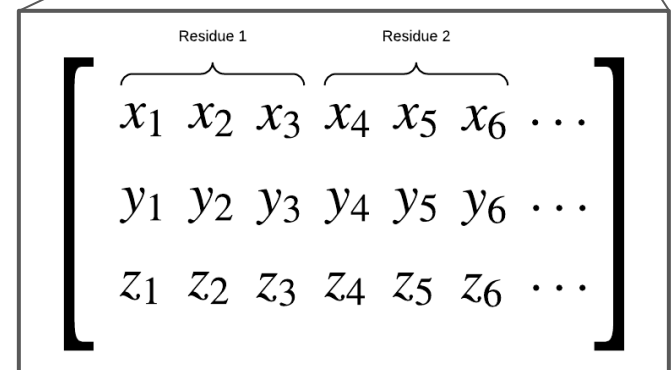


Recurrent Geometric Networks (RGNs)

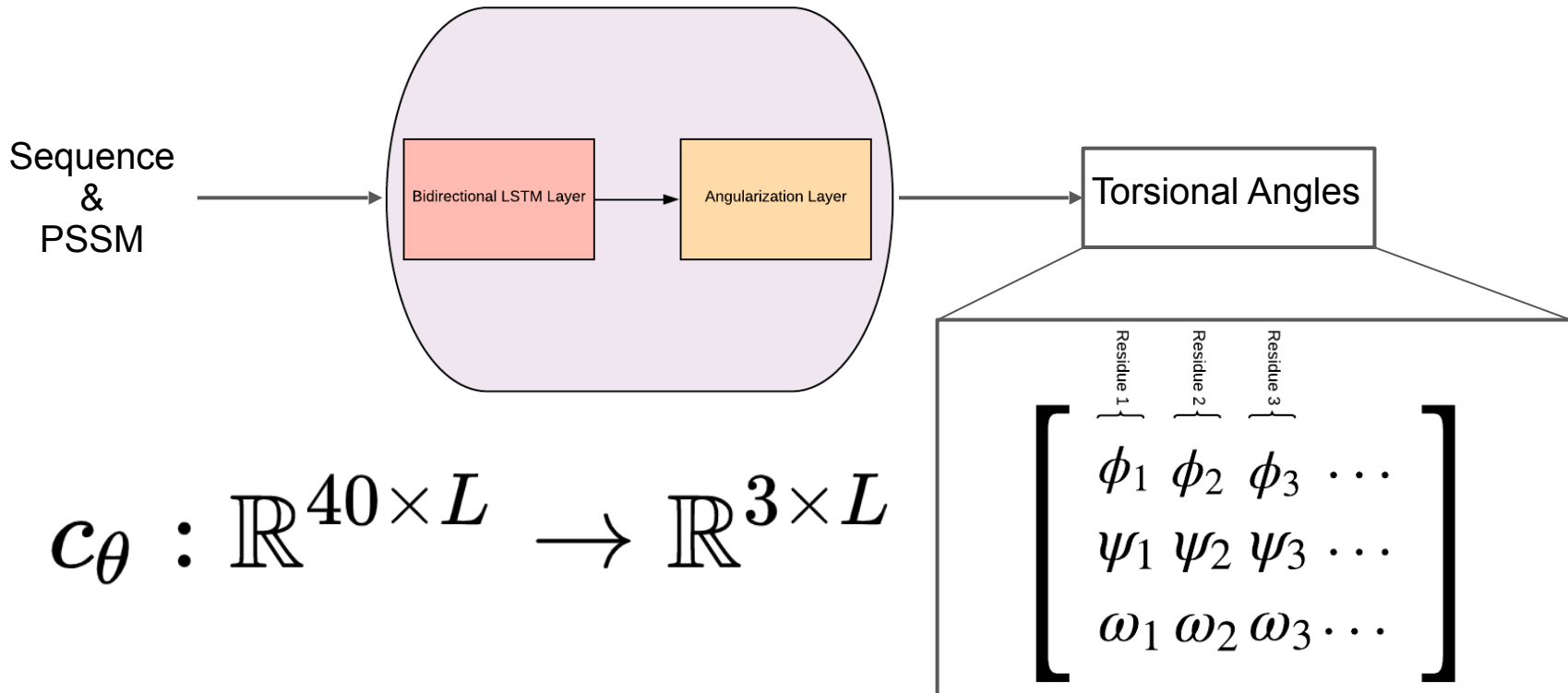


$$f_{\theta} : \mathbb{R}^{40 \times L} \rightarrow \mathbb{R}^{3 \times 3L}$$

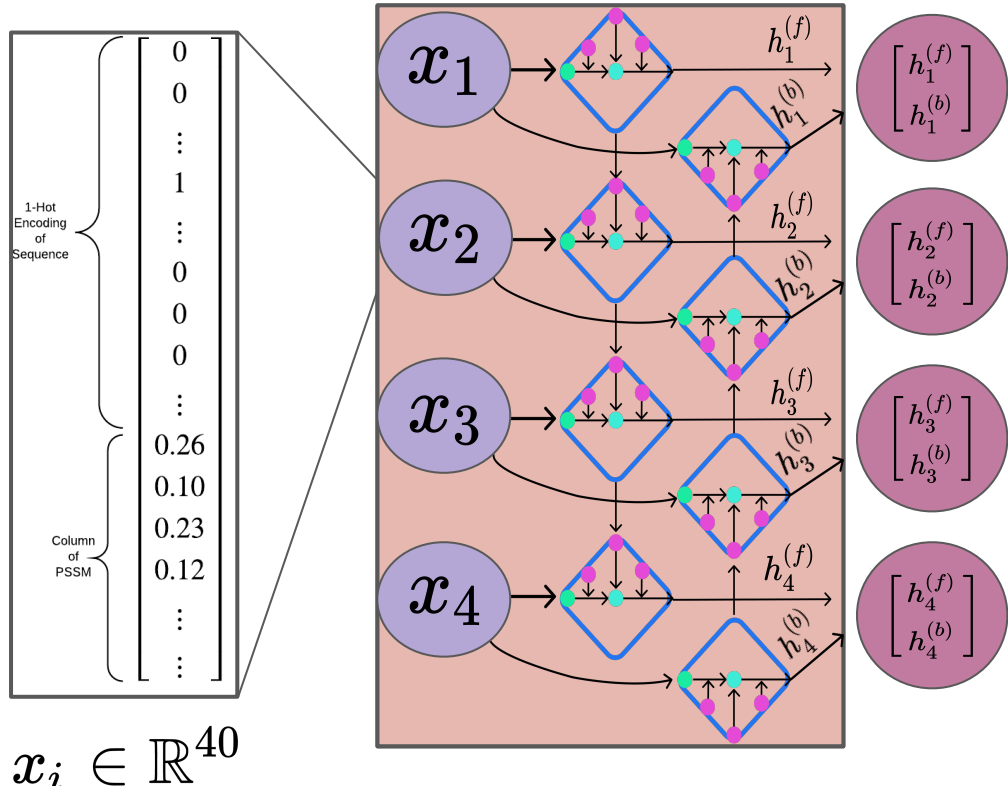
L = Sequence Length



Computation Stage



Bidirectional LSTM Layer

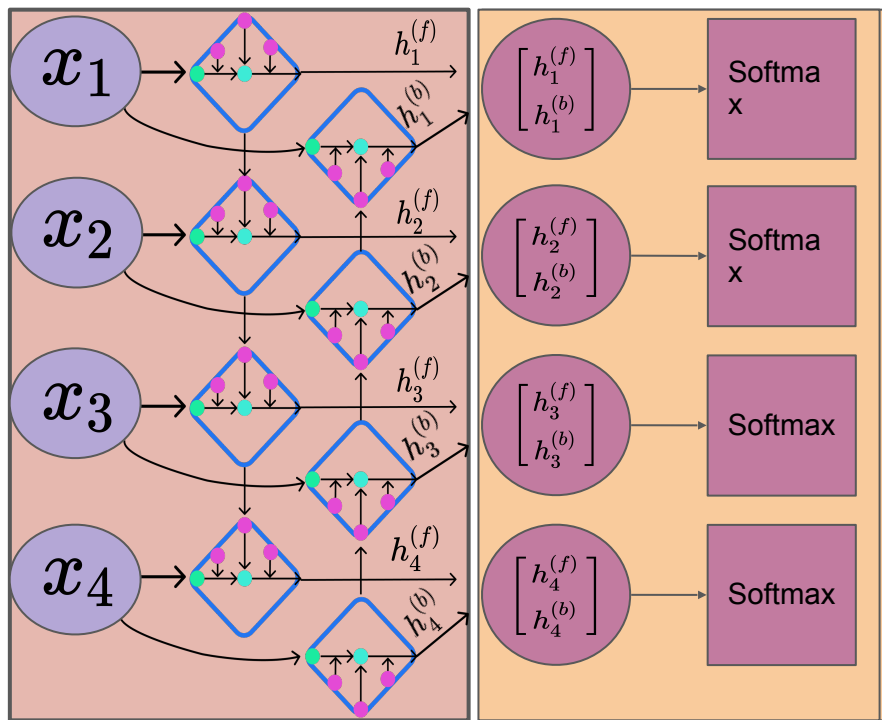


$x_i = \text{ith residue}$

$$h_i^{(f)}, h_i^{(b)} \in \mathbb{R}^{20} \quad \begin{bmatrix} h_i^{(f)} \\ h_i^{(b)} \end{bmatrix} \in \mathbb{R}^{40}$$

$$b_\theta^{(i)} : \mathbb{R}^{40} \rightarrow \mathbb{R}^{40}$$

Angularization Layer: Torsion Alphabet Probability Weight Generation

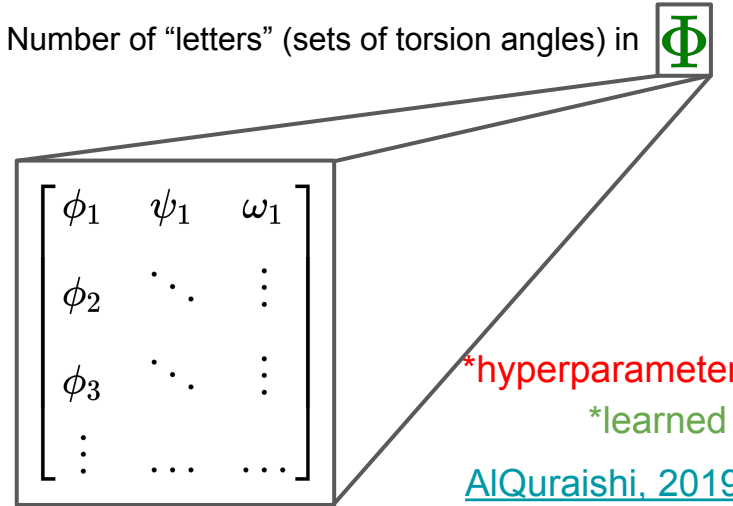


$$p_i = \text{softmax}(\mathbf{W}_\alpha [h_i^{(f)}, h_i^{(b)}] + \mathbf{b}_\alpha)$$

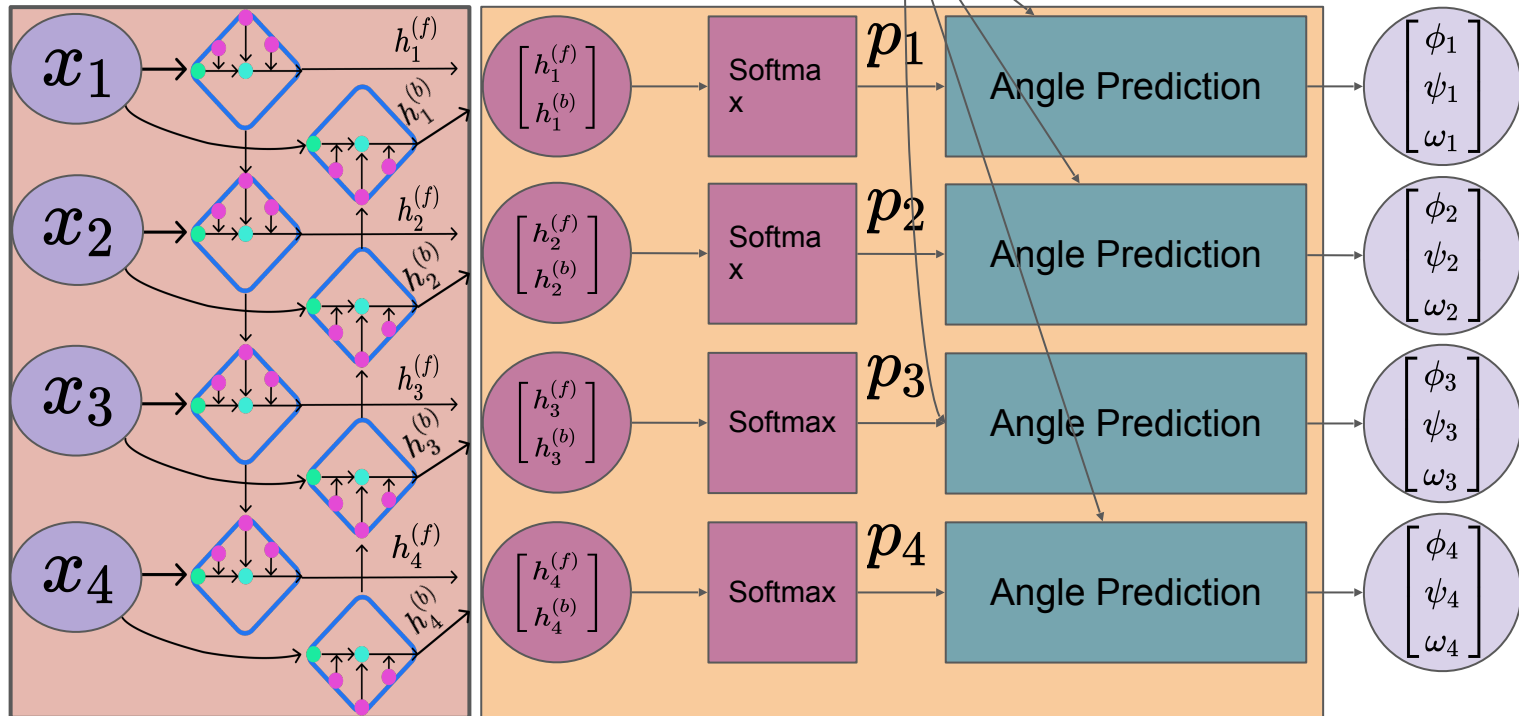
$$p_i \in \mathbb{R}^M \quad \Phi \in \mathbb{R}^{M \times 3}$$

Φ = Alphabet of sets of torsion angles

M = Number of “letters” (sets of torsion angles) in $\boxed{\Phi}$



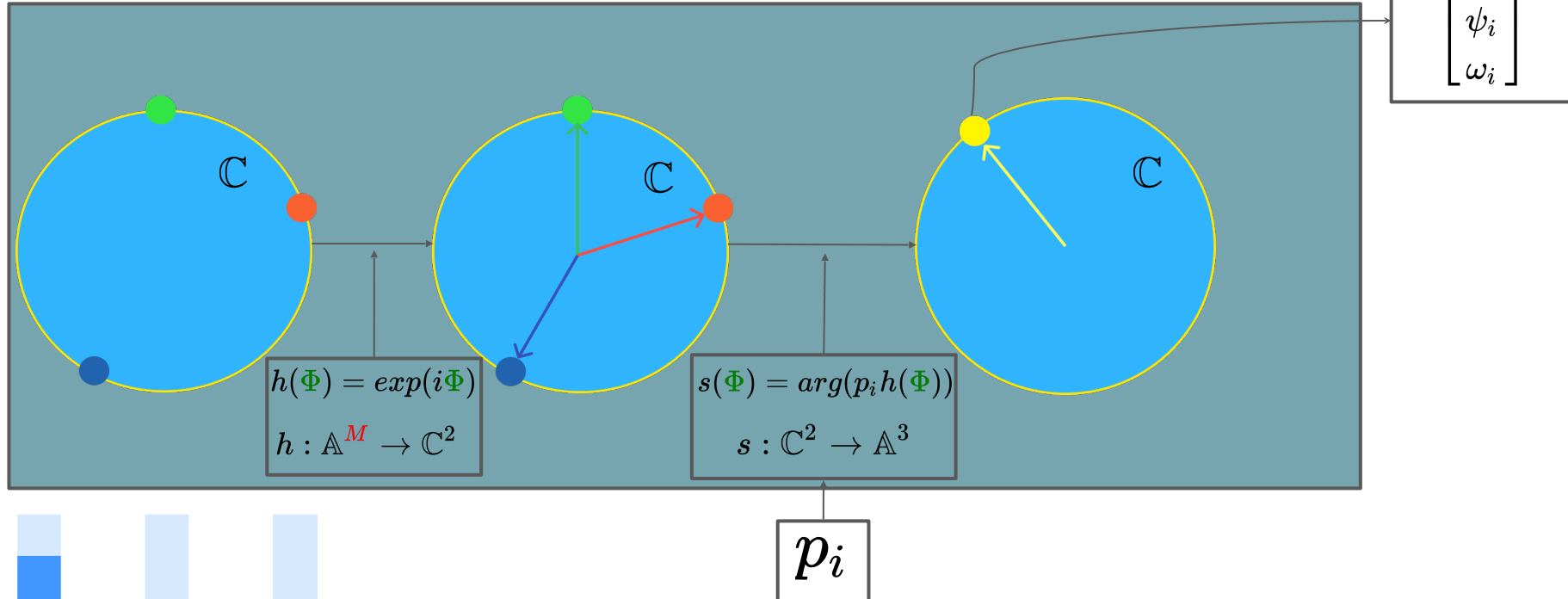
Angularization Layer



$$a_{\theta}^{(i)} : \mathbb{R}^{40} \rightarrow \mathbb{A}^3$$

*learned
AIQuraishi, 2019

Angularization Layer: Angle Prediction

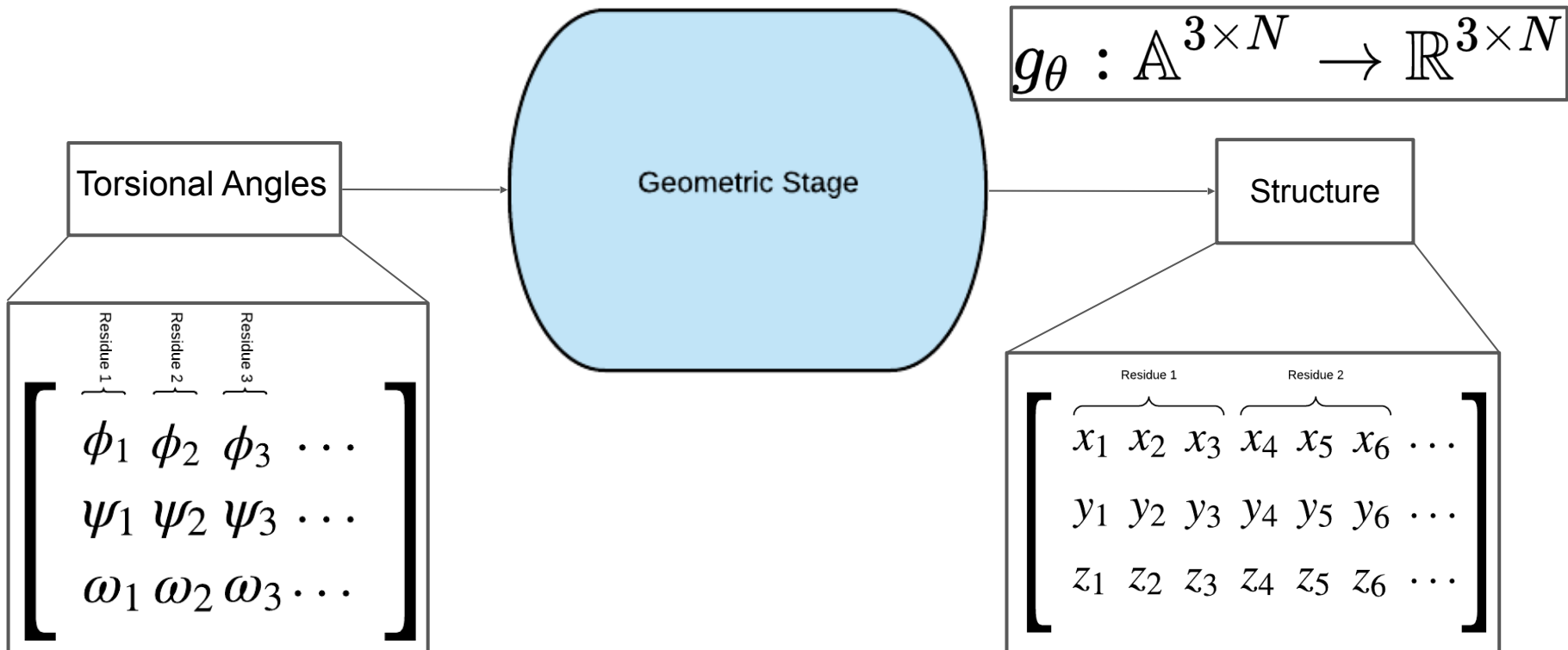


Φ_1 Φ_2 Φ_3

Note that for the sake of visual clarity, only 1 Cartesian vector is shown for each “letter”. In reality, there would be 3 Cartesian vectors for each letter (one for each torsional angle)

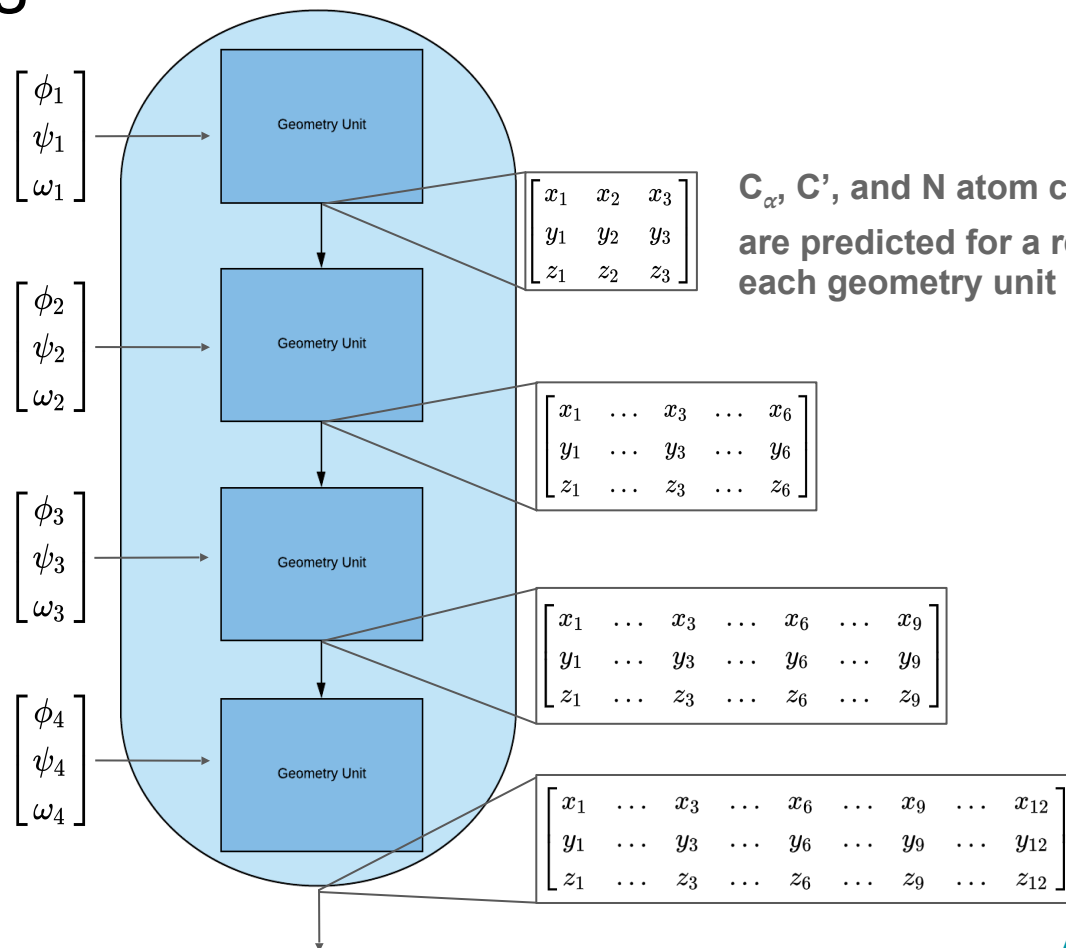
*hyperparameter
*learned
[AIQuraishi, 2019](#)

Geometric Stage



Geometric Stage

No Learning
Occurs Here



*hyperparameter

Geometric Unit

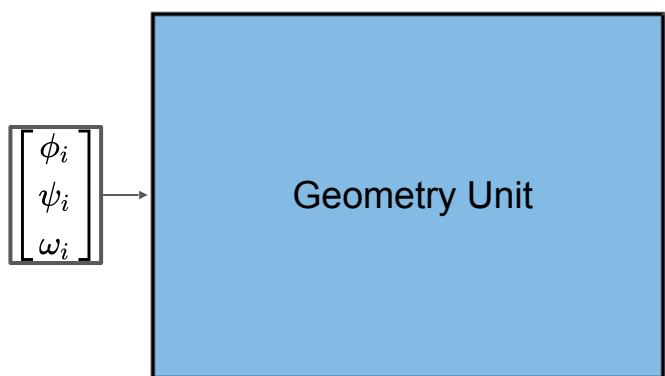
$$\begin{bmatrix} x_1 & \dots & x_{3(i-1)} \\ y_1 & \dots & y_{3(i-1)} \\ z_1 & \dots & z_{3(i-1)} \end{bmatrix}$$

$[r_0, r_1, r_2]$: fixed bond lengths

$[\theta_1, \theta_2, \theta_3]$: fixed bond angles

$[\psi_1, \psi_2, \psi_3]$: predicted dihedral angles

c_k : 3D coordinates of the k th atom in the protein



Denavit-Hartenberg
Transformation

$$\begin{bmatrix} x_1 & \dots & x_{3i} \\ y_1 & \dots & y_{3i} \\ z_1 & \dots & z_{3i} \end{bmatrix}$$

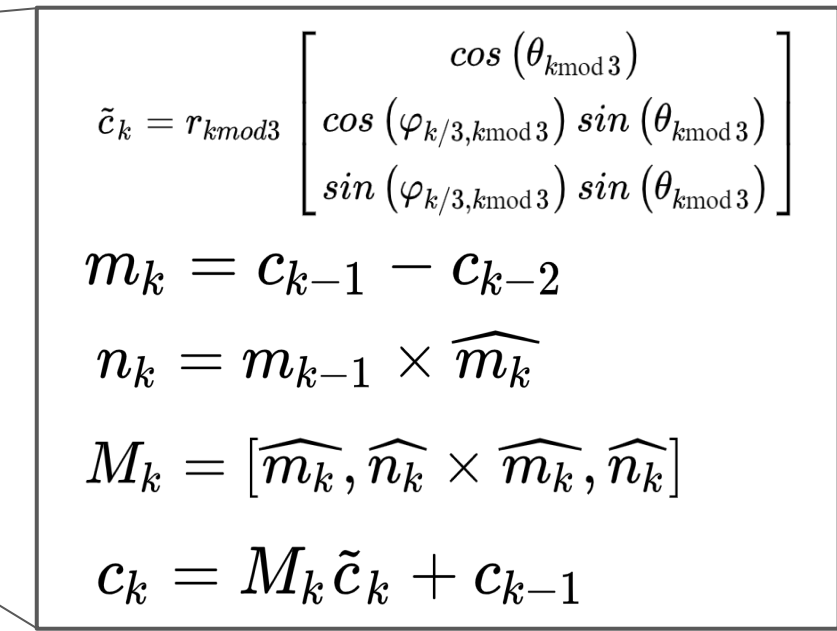
$$\tilde{c}_k = r_{k \bmod 3} \begin{bmatrix} \cos(\theta_{k \bmod 3}) \\ \cos(\varphi_{k/3, k \bmod 3}) \sin(\theta_{k \bmod 3}) \\ \sin(\varphi_{k/3, k \bmod 3}) \sin(\theta_{k \bmod 3}) \end{bmatrix}$$

$$m_k = c_{k-1} - c_{k-2}$$

$$n_k = m_{k-1} \times \widehat{m_k}$$

$$M_k = [\widehat{m_k}, \widehat{n_k} \times \widehat{m_k}, \widehat{n_k}]$$

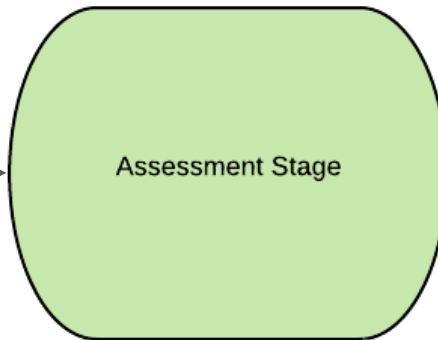
$$c_k = M_k \tilde{c}_k + c_{k-1}$$



Assessment Stage

Backpropagate and updated learned parameters

$$\begin{bmatrix} x_1 & \dots & x_{3L} \\ y_1 & \dots & y_{3L} \\ z_1 & \dots & z_{3L} \end{bmatrix}$$

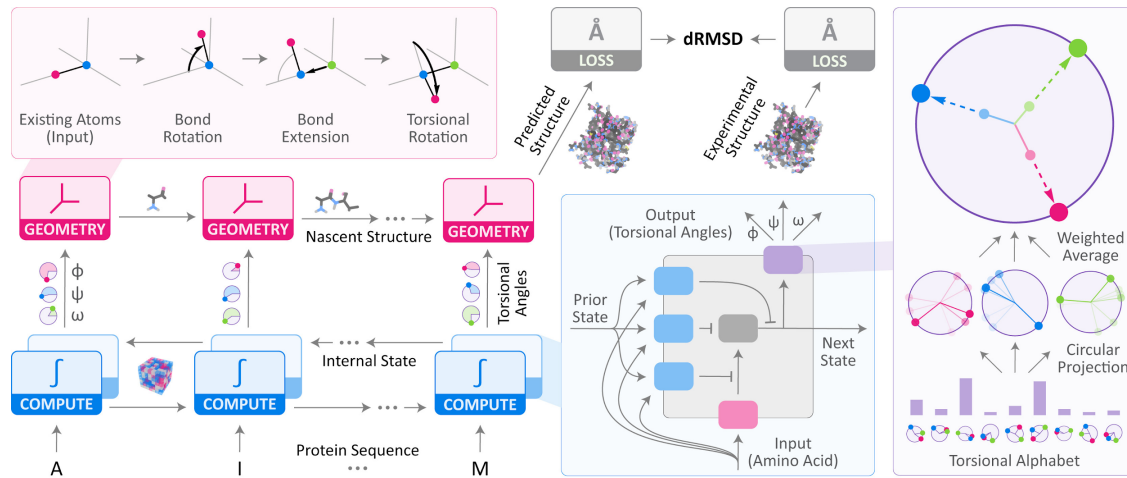


$$\tilde{d}_{j,k} = \|c_j - c_k\|_2 \quad d_{j,k} = \tilde{d}_{j,k}^{(\text{exp})} - \tilde{d}_{j,k}^{(\text{pred})}$$

$$\arg \min_{\theta} dRMSD = \frac{\|D\|_2}{L(L-1)}$$

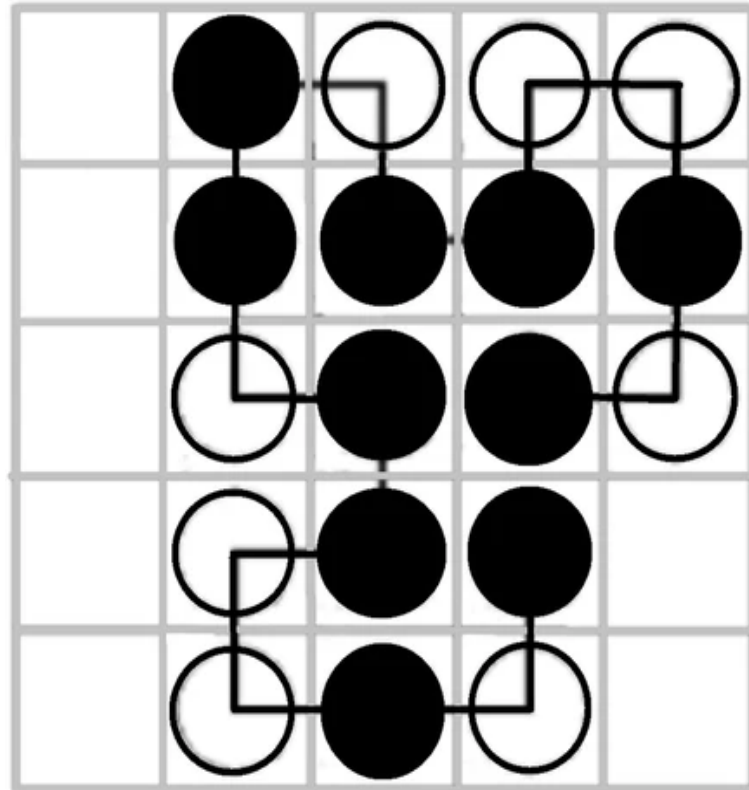
RGN Full Architecture

- 2 Bidirectional LSTM layers with 800 Compute Units per direction
- 0.5 input dropout rate
- Torsional Alphabet Size of 60
- LSTM and angularization layers both initialized with a uniform distribution
- ADAM optimizer with learning rate 0.001, $\beta_1 = 0.95$, $\beta_2 = 0.99$, and batch size of 32
- Gradient clipping with threshold of 5.0



DRL for 2D HP model

- Differs from the other methods in that the protein folding problem is modeled as a Deep Reinforcement Learning problem
- Uses 2D HP model, which treats every residue as either hydrophobic (H) or hydrophilic (P) and maps protein residues onto a 2D lattice
- Algorithm places residues one by one in lattice following a self-avoiding walk



DRL for 2D HP model cont.

- Goal is to minimize the free energy (the reward)
- Since proteins tend to form a hydrophobic core, a -1 reward (lowering the free energy) is given for each pair of non-consecutive H-residue pairs that end up as neighbors in the lattice
- Uses an actor-critic algorithm to learn the best policy
- Network uses three LSTM layers (each followed by a dropout layer) to approximate the Q-value function using a dueling architecture (the critic)
- Trained with an experience replay mechanism
- Goal is to place the current residue adjacent to the previous residue where the action space is {Up, Down, Left, Right}

DRL for 2D HP model

Pros:

- Novel use of DRL in protein folding
- Does not require labeled data unlike supervised learning
- Outperforms similar methods in less time

Cons:

- Reward function is very simplistic
- Only in two dimensions using a simplified lattice model
- Hydrophobicity has been binarized

CNR = Could not reach

Seq. #	ACO	Folding Zero	GA	EMC	ENLS	PER M	DRL
1	-9	-9	-9	-9	-9	-9	-9
2	-9	-8	-9	-9	-9	-9	-9
3	-8	-7	-8	-8	-8	-8	-8
4	-14	-13	-14	-14	-14	-14	-14
5	-23	-18	-23	-23	-23	-23	-23
6	-21	-18	-21	-21	-21	-21	-21
7	-36	-32	-34	-35	-36	-36	-36
8	-42	N/A	-37	-39	-39	-38	-42
9	-53	-48	CNR	-52	CNR	-53	-53
10	-50	N/A	CNR	CNR	CNR	-50	-50
11	-47	N/A	CNR	CNR	CNR	-48	-48

Comparison of Current SOA Methods

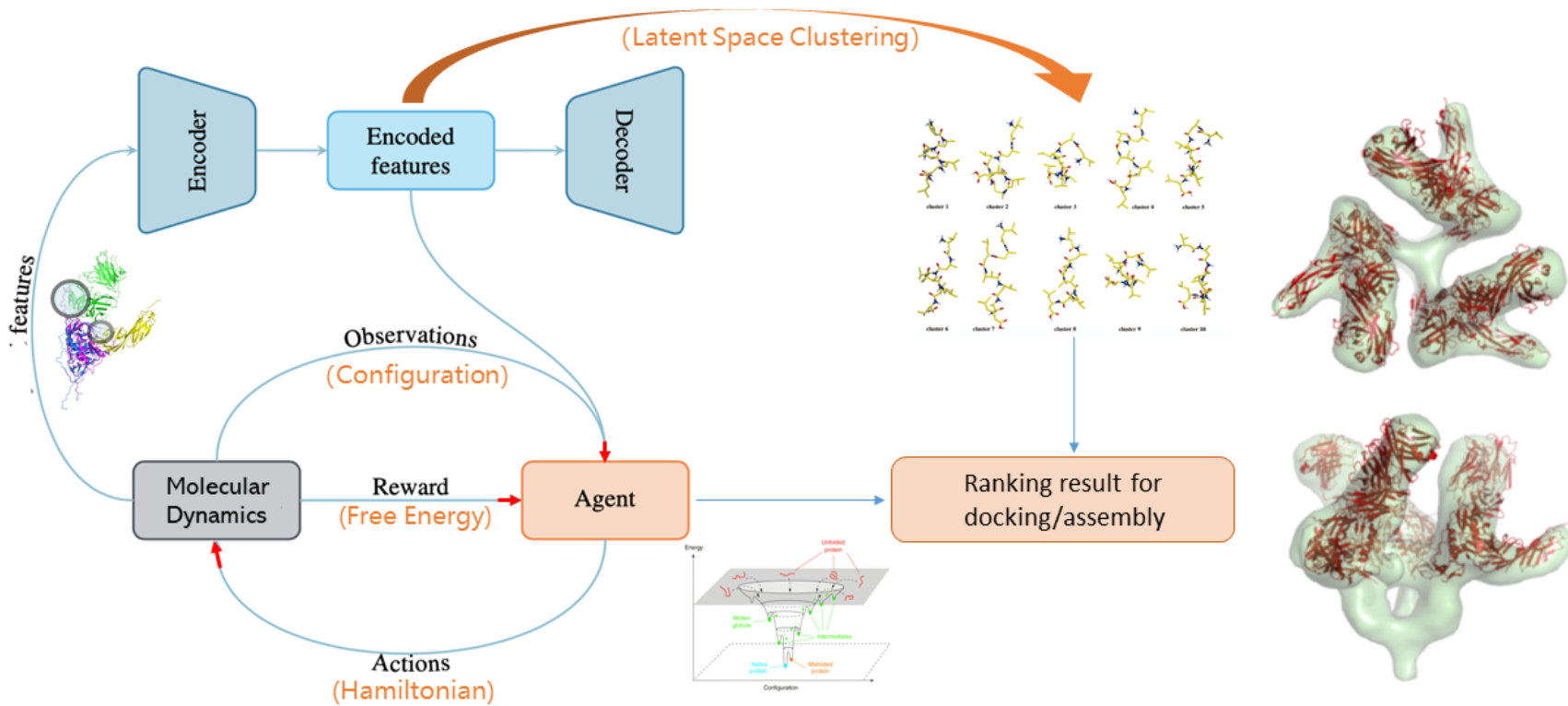
	RaptorX	AlphaFold	RGNs
Inputs	PSSM, MI, Predicted Secondary Structures, Predicted Solvent Accessibility, Pairwise Potential, CCMPred Coevolutionary Info	PSSMs (each from different software) and Potts model parameters	PSSM
Outputs	Distance Matrix	$L \times L \times 64$ distance distributions	Cartesian Coordinates
3D Model Determination	CNS	L-BFGS	Implicit
Energy Function	None	Constructed their own mean force potential	None
End-to-End Differentiable	No	No	Yes
Supervised/Unsupervised	Yes	Yes	Yes
Architecture	1D & 2D ResNets	2D ResNets	LSTMs
Folding Time	10 minutes to few hours on 20 CPUs	Not provided	Milliseconds with 1 GPU
Training Time	Hours	About 5 days	Weeks to months with 1 GPU
Secondary Structure Prediction	Predicted with a separate ResNet	Implicit	Implicit

TEMP OVERVIEW OF APPROACH SLIDE

- Our basic overview of approach
 - Part 1 (ODE + amber trajectory)
 - Part 2 (DRL)
 - Part 3 (VAE for MD)
- Challenges of approach and our proposed solutions to them

Our Approach

General Diagram of Our Approach



Challenges for our approach

Appendix

Multiple Sequence Alignment (MSA)

- A sequence alignment of 3 or more proteins such that homologous nucleotides or amino acids are located in the same column.
- Achieved by inserting gaps of varying length within the sequences, allowing homologous positions to be aligned with each other

HH01	1 MAPKKSTTKT TSKGKKPATS KGKEKSTSKA AIKKTTAKKE EASSKSYREL	50	HH01	201 S...RIVLKK YVKDTS...	250
HTB1	MSAK..... AEKKPASK A.....		HTB1	SQKSMSILNS FVNDIFE.....	.SKLTSSN
HTB2	MSSA..... AEKKPASK A.....		HTB2	SQKSMSILNS FVNDIFE.....	.RIATEASK
HTZ1		HTZ1	LQFPVGRIKR YLKRKA..T GTRVGSKAA IYLTAVLEYL TAEVLEAGN	
HTA2		HTA2	LTFPVGRVHR LLRGN... YAQRIGSGAP VYLTAVLEYL AAEIILEAGN	
HTA1		HTA1	LTFPVGRVHR LLRGN... YAQRIGSGAP VYLTAVLEYL AAEIILEAGN	
HMF1		HMF1	RRLARRGGVK	RISGLIY EEVRAVLKSF LESVIRDSVT
CSE4	MSSKQQIVSS AI...QSDS SGRSLSN... VNRLAGDQ... QSIND...	51 100	CSE4	SKIPFARLVK EVTDEFTTKD QDLRNQSMAI MALQEASEAY LVGLLEHTNL	
HHT1		HHT1	RKLPFQLRVR EIAQDFK... TDLRFQSSAI GALQESVEAY LVSLFEDTNL	
HHT2		HHT2	RKLPFQLRVR EIAQDFK... TDLRFQSSAI GALQESVEAY LVSLFEDTNL	
HTA2		251	251	300
HTA1		HH01	FDYL.FNSAIK...K CVENGELVQP KGP....SG II.....	
HMF1		HTB1	LAAYNKKSTI SAREIQTAVR LILPGELAKH AVS....EG TR.....	
HTM2		HTB2	LAAYNKKSTI SAREIQTAVR LILPGELAKH AVS....EG TR.....	
CSE4	..RALSLLQR TRATKNLFFP REERRRYE.. SSKSDLDIE..		HTZ1	AAKDLKVKR1 TPRHLQLAIR G..DDELDSL IR.ATIASGG VLPHINKALL	
HHT1		HTA2	AARDNKKTR1 IPRHLQLAIR N..DDELNLK LGNVTIAQGG VLPIHQNLL	
HHT2		HTA1	AARDNKKTR1 IPRHLQLAIR N..DDELNLK LGNVTIAQGG VLPIHQNLL	
HTA2		HMF1	YTEHAKRKT1 TS LDWVYALK R..QGRTLYG FG.....G	
HTA1		HTF2	YTEHAKRKT1 TS LDWVYALK R..QGRTLYG FG.....G	
HMF1		CSE4	LALHAKRIT1 MKKDMQLARR I..RGQFI~	
HTM2		HHT1	AAIHAKRVT1 QKKDIKLARR L..RGERS~	
CSE4	TDYED.. QA GNLEIETENE EEAEMETEVP APVRTHSYAL DRYVRQ...	101 150	HHT2	AAIHAKRVT1 QKKDIKLARR L..RGERS~	
HHT1 MA.RTK QTARKSTGGK APRKQ... LASK...		301	301	314
HHT2 MA.RTK QTARKSTGGK APRKQ... LASK...		HH01	.KLNNKKVKL ST~	
HTA2		HTB1	.AVTKYSSST QA~	
HTA1		HTB2	.AVTKYSSST QA~	
HMF1		HTZ1	LKVKEKKGSKK ~~~~	
HTM2		HTA2	PKKSAKTAKA SQEL	
CSE4 KR REKQRQKSLK RVEKKYTPSE LALYREIR... KYQSTDLLI	151 200	HTA1	PKKSAKTAKA SQEL	
HHT1 AA RKSAPSTGGV KKPHRYKPGT VALREIR... RFQKSTELLI		HHF1	~~~~~	
HHT2 AA RKSAPSTGGV KKPHRYKPGT VALREIR... RFQKSTELLI		HHF2	~~~~~	
CSE4	~~~~~		HHT1	~~~~~	
HHT1	~~~~~		HHT2	~~~~~	

Position-Specific Scoring Matrix (PSSM)

- Specifies the scores for observing particular amino acids at specific positions, based on the amino acid frequencies at every position of a MSA.
- $20 \times L$ Matrix. 20 corresponds to the amino acid alphabet and L corresponds to the sequence length
- The probability of seeing amino acid i in position j of the sequence is:

$$PPM_{ij} = \frac{c_{ij} + b}{k + 20(b)}$$

where c_{ij} is frequency of amino acid i at position j . b is a pseudocount added to account for possible examples of the pattern that are not represented in the training data. k is the number of sequences in the MSA.

- The matrix is then given by calculating the log odds ratios score of the observed given amino-acid at given position:

$$PSSM_{ij} = \log \frac{PPM_{ij}}{p_i} \quad \text{where } p_i \text{ is the background distribution of amino acid } i.$$

A Simple Sequence to PSSM Example

Sequences
 $k = 3$ $NIAGECC$
 $b = 1$ $NTEHEWI$
 $\forall i, p_i = 0.05$ $NITRGEW$

$$PPM_{ij} = \frac{c_{ij} + b}{k + 20(b)}$$

$$\Rightarrow PPM = \begin{bmatrix} N & 0.174 & 0.044 & 0.044 & 0.044 & 0.044 & 0.044 & 0.044 \\ T & 0.044 & 0.087 & 0.087 & 0.044 & 0.044 & 0.044 & 0.044 \\ \vdots & \vdots \\ E & 0.044 & 0.044 & 0.087 & 0.044 & 0.130 & 0.087 & 0.044 \\ G & 0.044 & 0.044 & 0.044 & 0.130 & 0.087 & 0.044 & 0.044 \end{bmatrix}$$

$$\downarrow PSSM_{ij} = \log \frac{PPM_{ij}}{p_i}$$

$$PSSM = \begin{bmatrix} N & 0.541 & -0.061 & -0.061 & -0.061 & -0.061 & -0.061 & -0.061 \\ T & -0.061 & 0.240 & 0.240 & -0.061 & -0.061 & -0.061 & -0.061 \\ \vdots & \vdots \\ E & -0.061 & -0.061 & 0.240 & -0.061 & 0.416 & 0.240 & -0.061 \\ G & -0.061 & -0.061 & -0.061 & 0.416 & 0.240 & -0.061 & -0.061 \end{bmatrix}$$

Neural ODEs ([Chen, et al. 2019](#))

We can represent Residual Networks in the form

$$h_t = h_{t-1} + f(h_{t-1}, \theta_t)$$

Viewing ResNets through a lense of differential equations, we can see that it resembles a discretization of Euler's Method, which is used to approximate continuous functions. Therefore, as we increase the number of layers in our ResNet (i.e. $t \rightarrow \infty$), the network approximates a continuous function governed by the differential equation

$$\frac{d\mathbf{h}(t)}{dt} = f(\mathbf{h}(t), t, \theta)$$

We can then frame finding the output as an initial value problem where $h(0)$ is the input layer and $h(T)$ is the output "layer" at some time T . We can then use an ODESolver to solve the network. Our loss is can thus be generally defined as

$$L(z(t_1)) = L(z(t_0) + \int_{t_0}^{t_1} f(\mathbf{z}(t), t, \theta) dt) = L(ODESolve(z(t_0), f, t_0, t_1, \theta))$$

Rather than backpropagate through the ODESolver (which would require a copious amount of memory), we can compute gradients with the *adjoint sensitivity* method where we solve the adjoint equation which results in constant space and linear time complexity.

Adjoint Sensitivity Method to Find the Gradient of Loss

In order to reverse auto-differentiate, we must first find the gradient of loss with respect to the hidden states which we will define as the *adjoint*, $\mathbf{a}(t) = \frac{d\mathbf{L}}{dz(t)}$. Its dynamics are given by

$$\frac{d\mathbf{a}(t)}{dt} = -a(t)^T \frac{\partial f(\mathbf{z}(t), t, \theta)}{\partial z}$$

which we can obtain with a call to an ODESolver. In order to find $\frac{d\mathbf{L}}{dz(t_0)}$, the ODESolver can be called again and must run backwards starting from $\frac{d\mathbf{L}}{dz(t_1)}$. Note that in order to find $\frac{d\mathbf{L}}{dz(t_0)}$, we need to recompute each hidden state together with the adjoints. Finally, we calculate the gradient of the loss with respect to the parameters with another integration.

$$\frac{d\mathbf{L}}{d\theta} = - \int_{t_1}^{t_0} a(t)^T \frac{\partial f(\mathbf{z}(t), t, \theta)}{\partial \theta} dt$$

In summary, we can calculate $a^T \frac{df}{dz}$ and $a^T \frac{df}{d\theta}$ with automatic differentiation. We can then calculate the integrals necessary for \mathbf{z} , \mathbf{a} , and $\frac{d\mathbf{L}}{d\theta}$ with a single ODESolve.

Control for bias Hamiltonian ([Wang, et al. 2020](#))

Simulating the positions of particles with conserved energy requires integrating the Hamiltonian equations of motion:

$$\frac{\partial p_i}{dt} = -\frac{\partial H}{\partial q_i}, \quad \frac{\partial q_i}{dt} = -\frac{\partial H}{\partial p_i}$$

where p_i and q_i are the momentum and position of the i -th particle, respectively. H is the Hamiltonian of the Systems; The Hamiltonian of a system specifies its total energy. For conservative systems it is given by:

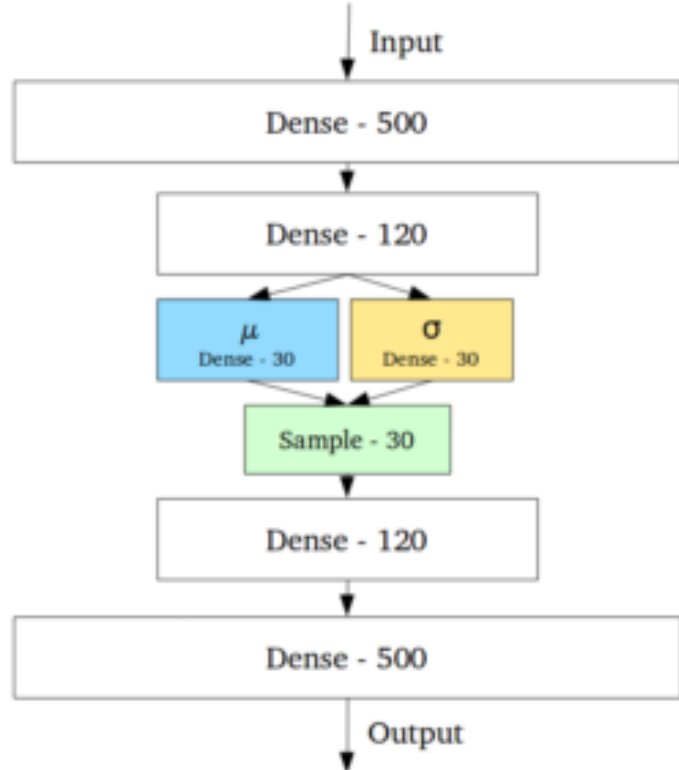
$$H(p, q) = U(q) + \sum_i \frac{\|p_i\|^2}{2m_i}$$

Where $U(q)$, is the potential energy for all the particles, and $\|p_i\|^2/(2m_i)$ is the kinetic energy of the i -th particle.

Simulating an entire system explicitly tracking all relevant degrees of freedom is computationally intractable in most cases. Typically, one is interested in a small subset of a system, such as a molecule or protein, and concerned only with the influence of the environment, also known as *bath*, on the system but not the details of the environment itself. For this reason, one usually incorporates an environment Hamiltonian H_b with coarse-grained macroscopic variables of interest into the original Hamiltonian: $H_{tot} = H + H_b$. The environment, and therefore H_b , can also be explicitly controlled and optimized in many complex physical processes.

Variational Autoencoder

- Unsupervised learning method
- Generally, autoencoders are to learn parameters such that the output is identical to the input
- However, input is passes through information bottleneck so network must learn the most salient information
- VAE's are stochastic versions of traditional autoencoders; it learns a distribution for each latent state attribute which is then sampled for the output



LSTMs (Long-Short-Term-Memory Networks)

- LSTMs allows the recurrent network to learn how to control the data flow with various gates and prevents vanishing gradient
- The **learned parameters** are the weight matrices, W_f, W_i, W_o , and W_c , and the bias vectors, b_f, b_i, b_o , and b_c

$$f_t = \sigma(W_f [x_t, h_{t-1}] + b_f)$$

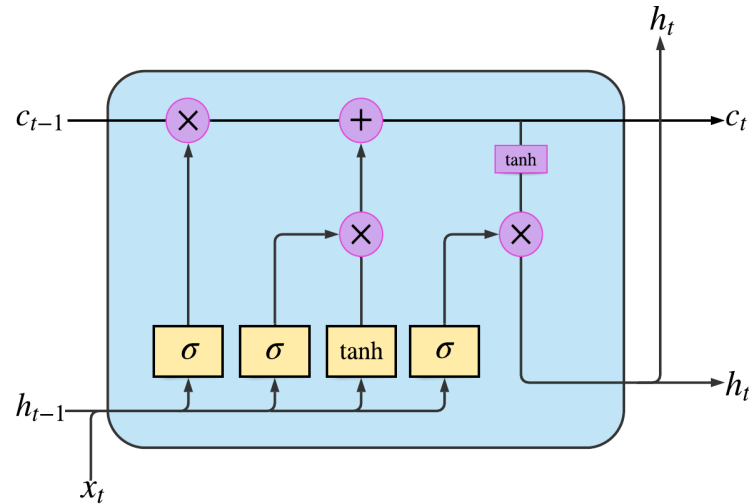
$$i_t = \sigma(W_i [x_t, h_{t-1}] + b_i)$$

$$o_t = \sigma(W_o [x_t, h_{t-1}] + b_o)$$

$$\tilde{c}_t = \tanh(W_c [x_t, h_{t-1}] + b_c)$$

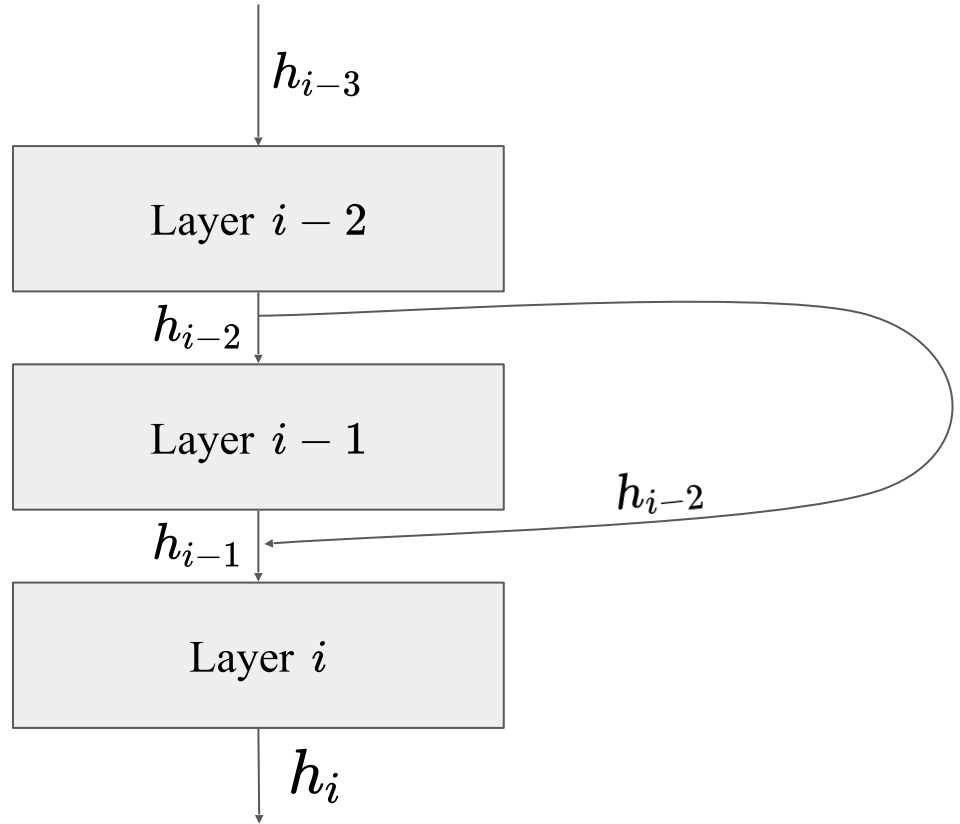
$$c_t = i_t \odot \tilde{c}_t + f_t \odot c_{t-1}$$

$$h_t = o_t \odot \tanh(c_t)$$



Residual Networks

$$h_i = \alpha(\mathbf{W}(h_{i-1}) + \mathbf{b}_i + h_{i-2})$$



*learned
[Wikipedia](#)

References

- [Aspuru-Guzik, A. \(2018\). Automatic Chemical Design Using a Data-Driven Continuous Representation of Molecules. *ACS Central Science*, 4, 268–276. doi: 10.1021/acscentsci.7b0057](#)
- [Mnih, V., Kavukcuoglu, K., Silver, D., Graves, A., Antonoglou, I., Wierstra, D., & Riedmiller, M.A. \(2013\). Playing Atari with Deep Reinforcement Learning. *ArXiv*, abs/1312.5602](#)
- [Wang, W., Axelrod, S., & Gómez-Bombarelli, R. \(2020\). Differentiable Molecular Simulations for Control and Learning. *ArXiv*, abs/2003.00868](#)
- [Rashid, M.A., Khatib, F., & Saltar, A. \(2015\). Protein preliminaries and structure prediction fundamentals for computer scientists. *ArXiv*, abs/1510.02775.](#)
- [Xu, J. \(2019\). Distance-based protein folding powered by deep learning. *Proceedings of the National Academy of Sciences*, 116\(34\), 16856–16865. https://doi.org/10.1073/pnas.1821309116](#)
- [Ching, T., Himmelstein, D. S., Beaulieu-Jones, B. K., Kalinin, A. A., Do, B. T., Way, G. P., Ferrero, E., Agapow, P. M., Zietz, M., Hoffman, M. M., Xie, W., Rosen, G. L., Lengerich, B. J., Israeli, J., Lanchantin, J., Woloszynek, S., Carpenter, A. E., Shrikumar, A., Xu, J., Cofer, E. M., ... Greene, C. S. \(2018\). Opportunities and obstacles for deep learning in biology and medicine. *Journal of the Royal Society. Interface*, 15\(141\), 20170387. https://doi.org/10.1098/rsif.2017.0387](#)
- [Jafari, R., Javidi, M.M. Solving the protein folding problem in hydrophobic-polar model using deep reinforcement learning. *SN Appl. Sci.* 2, 259 \(2020\). https://doi.org/10.1007/s42452-020-2012-0](#)
- [AlQuraishi, M. \(2019\). End-to-end differentiable learning of protein structure. *Cell Systems*, 8\(4\), 292–301.e3. https://doi.org/10.1016/j.cels.2019.03.006](#)
- [Chen, T.Q., Rubanova, Y., Bettencourt, J., & Duvenaud, D.K. \(2018\). Neural Ordinary Differential Equations. *ArXiv*, abs/1806.07366.](#)
- [Chowdhury, R., Beglov, D., Moghadasi, M., Paschalidis, I. Ch., Vakili, P., Vajda, S., Bajaj, C., & Kozakov, D. \(2014\). Efficient maintenance and update of nonbonded lists in macromolecular simulations. *Journal of Chemical Theory and Computation*, 10\(10\), 4449–4454. https://doi.org/10.1021/ct400474w](#)
- [Chowdhury, R., & Bajaj, C. \(2010\). Multi-level grid algorithms for faster molecular energetics. *Proceedings of the 14th ACM Symposium on Solid and Physical Modeling*, 147–152. https://doi.org/10.1145/1839778.1839799](#)
- [Senior, A. W., Evans, R., Jumper, J., Kirkpatrick, J., Sifre, L., Green, T., Qin, C., Žídek, A., Nelson, A. W. R., Bridgland, A., Penedones, H., Petersen, S., Simonyan, K., Crossan, S., Kohli, P., Jones, D. T., Silver, D., Kavukcuoglu, K., & Hassabis, D. \(2020\). Improved protein structure prediction using potentials from deep learning. *Nature*, 577\(7792\), 706–710. https://doi.org/10.1038/s41586-019-1923-7](#)